Density Functional Theory for the Distribution of Small Ions around Polyions

Chandra N. Patra and Arun Yethiraj*

Theoretical Chemistry Institute and Department of Chemistry, University of Wisconsin, 1101 University Avenue, Madison, Wisconsin 53706

Received: March 26, 1999; In Final Form: May 12, 1999

A density functional theory is presented for the distribution of charged hard spheres (model for salt) around an infinite, rigid, and impenetrable charged cylinder (model for DNA or tobacco mosaic virus). The theory is based on a weighted density approach where the hard-sphere contribution to the one-particle correlation function is evaluated nonperturbatively using a position dependent effective density, and the ionic part is obtained through a second-order functional Taylor expansion around a uniform fluid. The theory is in good agreement with Monte Carlo simulations for the density distribution of monovalent, divalent, and mixed salts. For axial charge densities corresponding to DNA, the hypernetted chain integral equation theory is not as accurate as the density functional theory, but both liquid state approaches are superior to the Poisson−Boltzmann theory. For higher axial charge densities the density functional theory predicts interesting charge inversion effects that are absent in the nonlinear Poisson−Boltzmann theory.

I. Introduction

The interactions of DNA with its counterions and the supporting electrolyte are believed to play an important role in the conformational stability of the polyion and the ligand binding equilibria in solution,[1] as well as the hydrodynamic, transport, and molecular properties of DNA solutions.[2] The interactions between polyions and small ions are also of significance in many technologically important systems such as polyacrylates, polymethacrylates, polyvinylsulfonates, and polystyrenesulfonate solutions.[3] A detailed knowledge of the spatial distribution of small ions in the vicinity of a polyelectrolyte is therefore fundamental to a microscopic understanding of these polyelectrolyte solutions. In this article we present a density functional theory for the distribution of small ions around polyions and compare this theory to computer simulations and other theoretical approaches.

There have been many studies of the counterion distribution around DNA.[4] It has been popular to model the DNA as infinitely long, rigid, charged cylinder, although more complex models have also been investigated.[5] Most theoretical studies are based on two well known theories: the Counterion Condensation (CC) theory[6] and the Poisson−Boltzmann (PB) theory.[7,8]

In Manning's original formulation of the CC theory,[9] condensation was introduced as a mathematical device necessary to prevent the divergence of the phase integral of an infinite line charge under limiting law conditions. The utility of theoretical descriptions based on CC theory has been confirmed,[10] often at salt concentrations well above the expected range of applicability. Manning's second theory[11] of condensation was formulated to account for the observed persistence of counterion binding at moderate salt concentrations at an extent predicted in the limit of infinite dilution. Counterion condensation was derived from free energy minimization of a simple two state model for the counterions. The CC theory has been extensively applied in several problems including analyses of competitive binding equilibria.[12]

The Poisson−Boltzmann equation, in both its linear[13] (LPB) and nonlinear[14] (NLPB) form, has been extensively applied to study the counterion distribution around charged cylinders with[15] and without[16] added salt. In most cases, the so called cell model (CPB)[17] has been used, where the polyion and electrolyte are confined within a cylindrical cell and the rest of the solution enters solely through boundary conditions for the PB equation at the edge of the cell. The finite size of the cell mimics finite polyion concentrations, and the single polyion limit is reached for infinitely large cells. The CPB equation has been used to calculate the electrostatic free energy,[18,19] osmotic coefficients,[18] and the activity coefficient[20] of solutions of DNA and electrolyte. An independent way of calculating electrostatic free energy of polyelectrolyte solutions through LPB, NLPB, and CPB has also been developed.[21] All of the above mentioned studies neglect correlations between the small ions. The CC and PB theories are reviewed by Anderson and Record.[22]

The importance of correlations between small ions on the counterion distribution has been investigated using functional expansions, integral equations, and cluster expansions. Fixman[23] used functional expansions to study the impact of correlations on the PB equation. He found that the PB equation was quite accurate except at high salt conditions or high charge on the small ions. Other theoretical studies of correlation effects include those using integral equations,[24−28] cluster expansion techniques,[29−31] and a modified Poisson−Boltzmann (MPB) approach.[32,33] These studies all agree that the PB equation is sufficient for salts with monovalent ions at low to moderate concentrations (less than about 0.1 M) but that correlation effects are important for divalent or mixed salts and for high concentrations. These theories have been tested against computer simulations[34−39] and are reviewed elsewhere.[22,33,36]

An attractive approach to the study of nonuniform fluids is using density functional theory (DFT).[40,41] In this approach one starts with a grand free energy as a functional of the density distribution. A minimization of the functional with respect to

* E-mail: yethiraj@chem.wisc.edu.

10.1021/jp991062i CCC: $18.00
Published on Web 07/02/1999

variations in the density distribution gives both the density distributions and the free energy. The advantages of this approach are that the density distributions can be easily calculated with the chemical potential of the small ions held fixed. Density functional theory has been widely applied to the structure of nonuniform simple liquids,[42] the freezing of liquids,[43] the liquid surface,[44] and nonuniform ionic[45,46] and dipolar[47,48] fluids. The successful application of nonperturbative approaches to DFT has led to the development of weighted density approximation (WDA) techniques which have been applied to simple fluids,[49,50] ionic,[51,52] and dipolar[47,48] fluids, and also for polymers.[53]

In this paper, we investigate a partially perturbative approach of DFT to the polyelectrolyte system where the hard sphere contribution to the excess free energy is calculated through a nonperturbative WDA and the electrical contribution is calculated by perturbation with respect to the uniform fluid. We find that the DFT is in good agreement with simulations for the density distribution of monovalent, divalent, and mixed salts around charged cylinders. For monovalent salts, the DFT, PB, and HNC theories are all quite accurate, but for divalent and mixed salts the DFT is more accurate than the other approaches.

For high axial charge densities on the cylinder, the DFT predicts interesting correlation and charge reversal effects. At low salt concentrations the DFT predicts a significantly greater accumulation of both counterions and co-ions near the DNA when compared to the PB approach. At intermediate and high salt concentrations the DFT predicts significant charge reversal, where at intermediate and large distances the electrostatic potential is always positive even though the cylinder charge is negative. These effects are not seen in the PB theory. Unfortunately we were unable to get converged solutions to the HNC theory in these cases.

The rest of this paper is organized as follows. The theory is described in section II, results are presented in section III, and a few concluding remarks are presented in section IV.

II. Theoretical Formulation

A. Molecular Model. The polyion is modeled as an infinite, isolated, rigid cylinder bearing a uniform axial charge density given by

$$\xi = \frac{\beta_0 e^2}{\epsilon b} \tag{1}$$

where e is the electron charge, b is the length per electronic unit of charge (inverse of linear charge density), $\beta_0 = (k_B T)^{-1}$, k_B is Boltzmann's constant, T is the temperature, and ϵ is the dielectric constant of the pure solvent, modeled as a uniform dielectric continuum with $\epsilon = 78.358$ (characterizing water). Throughout this work we set $T = 298.15$ K, $\xi = 4.2$, and $b = 1.7$ Å, which are the accepted values for double-stranded DNA.[22] The small ions (with α denoting the species) are modeled using the restricted primitive model (RPM), i.e., they are charged hard spheres of equal diameter, $d_\alpha = 4$ Å, and charge q_α. The DNA is impenetrable to the ions with a distance of closest approach of 10 Å, i.e., the DNA radius is $R = 8$ Å.

B. Density Functional Theory. In density functional theory one starts with an expression for the grand free energy, Ω, as a functional of the singlet density profiles, $\rho_\alpha(\mathbf{r})$, of each of the species, α. At equilibrium the grand free energy is minimal with respect to variations in the density profiles, i.e.,

$$\frac{\delta\Omega}{\delta\rho_\alpha(\mathbf{r})} = 0 \tag{2}$$

for each α, and this condition is used to determine the density profiles and the free energy.

The grand potential functional is related to the Helmholtz free energy functional through a Legendre transform

$$\Omega[\{\rho_\alpha\}] = F[\{\rho_\alpha\}] + \sum_\alpha \int d\mathbf{r}[u_\alpha(\mathbf{r}) - \mu_\alpha]\rho_\alpha(\mathbf{r}) \tag{3}$$

where $u_\alpha(\mathbf{r})$ is the external field (due to the DNA) acting on the atoms of species α, μ_α is the chemical potential of the αth component, and $\{\rho_\alpha\}$ is the set of all density profiles.

The functional $F[\{\rho_\alpha\}]$ is generally expressed as the sum of an ideal gas and an excess part. The ideal gas part is known exactly, and approximations must be developed for the excess part. With this decomposition, $F[\{\rho_\alpha\}]$ may be written as

$$F[\{\rho_\alpha\}] = k_B T \sum_\alpha \int d\mathbf{r}\rho_\alpha(\mathbf{r})\{\ln[\rho_\alpha(\mathbf{r})\lambda_\alpha^3] - 1\} + F_{ex}[\{\rho_\alpha\}] \tag{4}$$

where F_{ex} is the excess free energy functional and λ_α is the de Broglie wavelength of the αth component. The main approximation in any density functional theory is the choice of F_{ex}. In developing such approximations, it is useful to recall the fact that F_{ex} defines the direct correlation functions of different order through functional derivatives, the most important ones being the first- and second-order correlation functions defined, respectively, as

$$c_\alpha^{(1)}(\mathbf{r_1}) = -\beta_0 \frac{\delta F_{ex}[\{\rho_\alpha\}]}{\delta\rho_\alpha(\mathbf{r_1})} \tag{5}$$

and

$$c_{\alpha\beta}^{(2)}(\mathbf{r_1},\mathbf{r_2}) = -\beta_0 \frac{\delta^2 F_{ex}[\{\rho_\alpha\}]}{\delta\rho_\alpha(\mathbf{r_1})\delta\rho_\beta(\mathbf{r_2})} = \frac{\delta c_\alpha^{(1)}(\mathbf{r_1})}{\delta\rho_\beta(\mathbf{r_2})} \tag{6}$$

Without loss of generality, we decompose F_{ex} into three terms:

$$F_{ex}[\{\rho_\alpha\}] = F_{ex}^{hs}[\{\rho_\alpha\}] + \frac{1}{2}\int\int d\mathbf{r_1}d\mathbf{r_2}\sum_{\alpha\beta} q_\alpha q_\beta \frac{\rho_\alpha(\mathbf{r_1})\rho_\beta(\mathbf{r_2})}{|\mathbf{r_1} - \mathbf{r_2}|} + F_{ex}^{el}[\{\rho_\alpha\}] \tag{7}$$

where the first term on the right hand side is the hard sphere contribution, the second term is the direct Coulomb contribution (in the van der Waals type approximation), and the third term is the residual electrostatic contribution. Equation 7 is formally exact, but expressions for the excess free energy functionals are not known. In this work we use the weighted density approximation for F_{ex}^{hs} and use a perturbative scheme for F_{ex}^{el}. Following Patra and Ghosh[46] we develop approximations for the direct correlation functions rather than the free energy functional itself. Note that the NLPB equation is recovered if we set $F_{ex}^{hs} = F_{ex}^{el} = 0$. In this limit, eq 7 therefore provides a simple expression for the free energy in the NLPB approximation, which may be compared to the development of Sharp and Honig.[21]

Before stating our approximations for the excess free energy functional, some manipulations are instructive. A formal minimization of the grand free energy gives

$$\mu_\alpha = u_\alpha(\mathbf{r}) + \frac{\delta F[\{\rho_\alpha\}]}{\delta \rho_\alpha(\mathbf{r})} \tag{8}$$

If one considers the cylindrical symmetry of the present system, the density variations occur only in radial direction (x), and one can simplify the above equation to:

$$\mu_\alpha = u_\alpha^{hs}(x) + q_\alpha \psi(x) + \frac{1}{\beta_0}\{\ln \rho_\alpha(x)\lambda_\alpha^3 - c_\alpha^{(1)hs}(x;[\{\rho_\alpha\}]) - c_\alpha^{(1)el}(x;[\{\rho_\alpha\}])\} \tag{9}$$

where $u_\alpha^{hs}(x)$ is the hard-sphere potential and $\psi(x)$ is the mean electrostatic potential due to the surface charge and the ionic distribution. The quantities $c_\alpha^{(1)hs}(x;[\{\rho_\alpha\}])$ and $c_\alpha^{(1)el}(x;[\{\rho_\alpha\}])$ denote, respectively, the hard-sphere and electrical-hard-sphere coupling contributions to the first order correlation function and are defined through expressions similar to equation 5.

The electrostatic potential $\psi(x)$ is obtained from a solution of the corresponding Poisson−Boltzmann equation in cylindrical geometry, which gives

$$\psi(x) = -\frac{4\pi}{\epsilon}[R\sigma \ln x + \ln x \int_R^x dt\, t \sum_\alpha q_\alpha \rho_\alpha(t) + \int_x^\infty dt\, t \sum_\alpha q_\alpha \rho_\alpha(t)] \tag{10}$$

where σ is the surface charge density defined as

$$\sigma = \frac{e}{2\pi R b} \tag{11}$$

Using the electroneutrality condition, given by

$$\int_R^\infty dt\, t \sum_\alpha q_\alpha \rho_\alpha(t) = -R\sigma \tag{12}$$

equation (10) can be simplified to

$$\psi(x) = \frac{4\pi}{\epsilon}\int_x^\infty dt\, t \ln\left(\frac{x}{t}\right)\sum_\alpha q_\alpha \rho_\alpha(t) \tag{13}$$

The free energy functional is completely specified by expressions for $c_\alpha^{(1)hs}(x;[\{\rho_\alpha\}])$ and $c_\alpha^{(1)el}(x;[\{\rho_\alpha\}])$ for a nonuniform density distribution. In fact we only need expressions for the difference between these correlation functions and the corresponding correlation functions for a bulk fluid, as can be seen if we rewrite eq 9 by evaluating the chemical potential, μ_α using the bulk phase density ρ_α^0 and substituting this result into eq 9. This gives

$$\rho_\alpha(x) = \rho_\alpha^0 \exp\{-\beta_0 q_\alpha \psi(x) + c_\alpha^{(1)hs}(x;[\{\rho_\alpha\}]) - c_\alpha^{(1)hs}([\{\rho_\alpha^0\}]) + c_\alpha^{(1)el}(x;[\{\rho_\alpha\}]) - c_\alpha^{(1)el}([\{\rho_\alpha^0\}])\} \tag{14}$$

which determines the density distribution of small ions in the region $x > (R + d_\alpha/2)$. In the absence of explicit expressions for $c_\alpha^{(1)hs}(x;[\{\rho_\alpha\}])$ and $c_\alpha^{(1)el}(x;[\{\rho_\alpha\}])$, we propose an approximation scheme based on the knowledge of these correlation functions for a uniform fluid. Our approach is similar to that of Patra and Ghosh.[46]

In the present work, because the hard-sphere diameters of anions and cations are equal, the procedure used for the calculation of $c_\alpha^{(1)hs}(x;[\{\rho_\alpha\}])$ is identical to that for a one-component hard-sphere liquid, and we evaluate this function using weighted density approximation (WDA) of Denton and Ashcroft.[54] In this approach the $c_\alpha^{(1)hs}(x;[\{\rho_\alpha\}])$ for a nonuniform system is evaluated using the expression for a uniform system at a weighted density, i.e.,

$$c_\alpha^{(1)hs}(x;[\{\rho_\alpha\}]) = \tilde{c}^{(1)hs}(\bar{\rho}(x)) \tag{15}$$

where the $\tilde{c}$ denotes the correlation function of a uniform fluid, the weighted density is defined by

$$\bar{\rho}(x) = \int dt\, t w^{hs}(x, t; \bar{\rho}(x))[\sum_\alpha \rho_\alpha(t)] \tag{16}$$

and $w^{hs}(x, t)$ is the weighting function, discussed below. Note that because the species have identical hard-sphere diameters, $c_\alpha^{(1)hs}(x;[\{\rho_\alpha\}])$ is a function only of the total density of sites.

The weighting function is determined by requiring that the first functional derivative of eq 15 with respect to the densities $\rho_\alpha(x)$ or $\rho_\beta(x)$ should yield the exact appropriate two-particle correlation functions in the uniform limit. This gives

$$w^{hs}(x, t; \bar{\rho}(x)) = \frac{\int_{-z_0}^{z_0}\int_0^{\phi_0} dz\, d\phi \tilde{c}^{(2)hs}(s;\bar{\rho}(x))}{\partial \tilde{c}^{(1)hs}/\partial \rho|_{\bar{\rho}(x)}} \tag{17}$$

where the interparticle distance s can be expressed in cylindrical coordinates as

$$s^2 = z^2 + x^2 + t^2 - 2xt\cos\phi \tag{18}$$

and the integration limits z_0 and ϕ_0 are given by

$$z_0 = (d_\alpha^2 - x^2 - t^2 + 2xt\cos\phi)^{1/2} \tag{19}$$

$$\phi_0 = \cos^{-1}\left(\frac{x^2 + t^2 - d_\alpha^2}{2xt}\right) \tag{20}$$

In the above, we have used the mean spherical approximation (or Percus−Yevick) result, i.e., $\tilde{c}^{(2)hs}(s) = 0$ for $s > d_\alpha$.

We obtain the electrical contribution to the one-particle correlation function in eq 14 in a partially perturbative manner, i.e., by evaluating

$$c_\alpha^{(1)el}(x,[\{\rho_\alpha\}]) - c_\alpha^{(1)el}([\{\rho_\alpha^0\}]) = \sum_\beta \int dt\, t\, \tilde{c}_{\alpha\beta}^{(2)el}(x,t;[\{\rho_\alpha^0\}])(\rho_\beta(t) - \rho_\beta^0) \tag{21}$$

where

$$\tilde{c}_{\alpha\beta}^{(2)el}(x,t;[\{\rho_\alpha^0\}]) = \int_{-z_0}^{z_0}\int_0^{\phi_0} dz\, d\phi\, \tilde{c}_{\alpha\beta}^{(2)el}(s;[\{\rho_\alpha^0\}]) \tag{22}$$

The theory is now completely specified by approximations for the pair direct correlation functions of the uniform fluid, which are readily available[55] in the mean spherical approximation, and explicit expressions for which are given below

$$c_{\alpha\beta}^{(2)hs}(s;\rho_0) = a_1 + a_2 s + a_3 s^3 \tag{23}$$

$$c_{\alpha\beta}^{(2)el}(s;\rho_0) = -\left(\frac{\beta_0 q_\alpha q_\beta}{\epsilon}\right)\left[2B - B^2 s - \frac{1}{s}\right] \tag{24}$$

valid for $s < d_\alpha$ and zero otherwise. In the above expressions

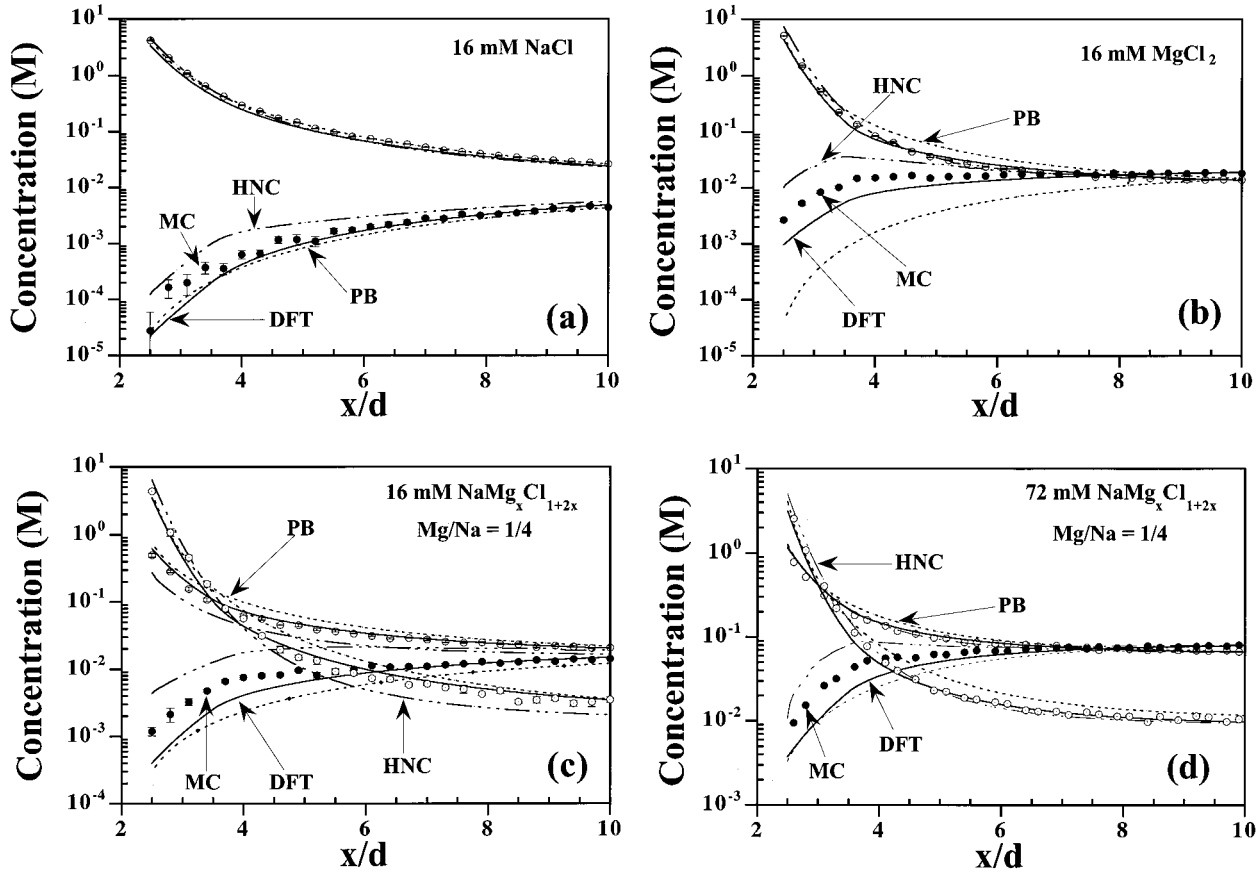

Figure 1. Concentration profiles for an NaCl/$MgCl_2$ salt around (negatively charged) DNA for: (a) pure 16 mM NaCl, (b) pure 16 mM $MgCl_2$, (c) 16 mM NaCl with $MgCl_2$ added so that the ratio of Mg^{2+} to Na^+ is 1:4, and (d) same as (c) but for 72 mM NaCl. The curves with a higher value near the DNA (compared to in the bulk) represent counterion concentration profiles and the other curves represent co-ion concentration profiles. Circles are simulation results[59] and lines are predictions of the DFT (—), PB (- - - -), and HNC (— - - - —) theories.

$$\eta = \frac{\pi}{6}\rho_0 d^3 \qquad \rho_0 = \sum_\alpha \rho_\alpha^0 \tag{25}$$

$$a_1 = \frac{2a_3}{\eta} = -\frac{(1+2\eta)^2}{(1-\eta)^4} \tag{26}$$

$$a_2 = 6\eta\frac{\left(1+\frac{\eta}{2}\right)}{(1-\eta)^4} \tag{27}$$

$$B = \frac{m+1-(1+2m)^{1/2}}{m} \tag{28}$$

$$m = \frac{4\pi\beta_0}{\epsilon}\sum_\alpha q_\alpha^2\,\rho_\alpha \tag{29}$$

C. Hypernetted Chain Integral Equation Theory. In cylindrical geometry, the Ornstein−Zernike (OZ) equation[56] takes the form (in Fourier space)[57]

$$\bar{h}_{p\alpha}(k) = \bar{c}_{p\alpha}(k) + \sum_\gamma \rho_\gamma^0\,\bar{c}_{p\gamma}(k)\hat{h}_{\gamma\alpha}(k) \tag{30}$$

where the overbars indicate two-dimensional Fourier transforms of circularly symmetric functions (Hankel transforms of order zero), carets indicate three-dimensional Fourier transforms of spherically symmetric functions, and the subscript p denotes polyion. We close eq 30 with the hypernetted chain (HNC) closure approximation. The density profiles of the ions are obtained from $\rho_\alpha(r) = \rho_\alpha^0(1 + h_{p\alpha}(r))$ where ρ_α^0 is the bulk density of species α. The correlation functions, $\hat{h}_{\beta\alpha}(k)$, for the pure salt case may be obtained by first solving the OZ equation for the pure salt case, i.e.,

$$\hat{h}_{\beta\alpha}(k) = \hat{c}_{\beta\alpha}(k) + \sum_\gamma \rho_\gamma^0\,\hat{c}_{\beta\gamma}(k)\hat{h}_{\gamma\alpha}(k) \tag{31}$$

with the HNC closure approximation. These integral equations are solved by standard Picard iteration techniques using the fast Fourier transforms, with the long-ranged part of the correlation functions evaluated analytically as described elsewhere.[28,58]

III. Results and Discussion

We first discuss ion distributions for pure 1:1 (NaCl), pure 2:1 ($MgCl_2$), and mixed 1:2:1 (NaCl/$MgCl_2$) salts at concentrations of 16 mM, 72 mM, and 239 mM, in each case. We present results for parameters that are identical to those employed in recent computer simulations[59] in order to test predictions of the various theories. These parameter values are given by T = 298.15 K, ϵ = 78.358, ξ = 4.2, R = 8 Å, and d_α = 4 Å. Subsequently, we investigate the effect of linear charge density for 2:1 and 2:2 salts at conditions where simulation results are not available.

Figure 1a−d depicts concentration profiles of co-ions and counterions as a function of radial distance from the DNA for various total salt concentrations and NaCl mole fractions. In all cases there is a significant accumulation of counterions near the DNA (note that the ordinates use a logarithmic scale) which results in a local concentration in the molar range which is several orders of magnitude higher than the bulk salt concentra-

tion. This is accompanied by a depletion of co-ions near the DNA by a similar amount.

In the case of pure NaCl (Figure 1a) the Na^+ concentration profiles predicted by all of the theories (DFT, HNC, PB) are almost identical to each other and agree quite well with the MC results. Differences between theoretical predictions are observed in the Cl^- concentration profiles, where the DFT and PB approaches are quite accurate when compared to the simulations but the value of the concentration near the DNA obtained from the HNC theory is higher in magnitude. Even though the concentration of co-ions near the DNA is rather small ($\sim$ 0.1 mM), this difference could be significant in biological experiments where the concentrations of supporting electrolytes are also of this order.

There is more structure in the concentration profiles of the 2:1 salt ($MgCl_2$) when compared to similar profiles of NaCl. In Figure 1b, the small ion distributions decrease rapidly to the bulk value within a distance of about 8*d*. The Cl^- concentration near the DNA is about two orders of magnitude higher than in the NaCl case, and the profile is relatively flat for distances greater than about 4*d*. These features may be attributed to the increase of effective screening of the cylindrical polyion charge by the presence of divalent (as opposed to monovalent) counterions. In addition there is a cusp in the concentration profiles at distances of $r = R + 3d_\alpha/2$ which we attribute to layering due to hard-sphere exclusions. The HNC and DFT approaches reproduce all of the qualitative features observed in the simulations, but the PB theory does not. For example the PB theory misses the hard-sphere-induced structure and the crossing of the Mg^{2+} and Cl^- concentration profiles. In fact it is not in good agreement with the simulations even for the counterion concentration profile. The HNC theory is more accurate than the PB, although it significantly overestimates the value of the Cl^- concentration near the DNA. The DFT is clearly the most accurate of the theories tested, and is in good agreement with the simulations at all distances.

In mixed 1:2:1 ($NaCl/MgCl_2$) salts, the introduction of a small amount of divalent (Mg^{2+}) counterions leads to the reduction of the concentration of monovalent counterions (Na^+) around the DNA, when compared to the pure NaCl case. This is seen in Figures 1c and 1d which depict the concentration profiles for a mixed $NaCl/MgCl_2$ salt with 16 and 72 mM NaCl, respectively, and added $MgCl_2$ so that the ratio of Na^+ to Mg^{2+} concentrations is 4. The exclusion of co-ions (Cl^-) around DNA in the presence of divalent counterion (Mg^{2+}) is much less than in the case of pure NaCl salt. Both of these effects may be attributed to the accumulation of Mg^{2+} counterions near the DNA, which leads to exclusion of Na^+ counterions and a reduction of the effective charge of the DNA felt by the co-ions. The relative performance of the DFT, HNC, and PB theories is intermediate to that observed in the limiting cases of pure 1:1 and 2:1 salts, and although the DFT is more accurate than the other two approaches, quantitative differences are smaller than in the pure $MgCl_2$ case. Interestingly, as the overall concentration is increased, the PB theory becomes more competitive with the DFT. This may be because the the small ions screen the electrostatic interactions with the DNA, thus making the mean field approximations in the PB more appropriate.

Figure 2 compares the mean electrostatic potential from the PB and DFT theories for salt concentrations ranging from 16 to 239 mM and various NaCl mole fractions. (Note that we plot $-\beta_0\psi(x)$ on the ordinate, and therefore a large positive value in Figure 2 corresponds to an attractive potential for a positive ion.) With increasing concentration or Mg^{2+} fraction, the mean electrostatic potential becomes less negative because of the increased strength of electrostatic interactions between the counterions and the DNA, i.e., the counterions screen the DNA charge and thus reduce the magnitude of the net electrostatic potential at larger distances. The PB theory always predicts an electrostatic potential of greater magnitude than the DFT, although the qualitative behavior in the two approaches is similar.

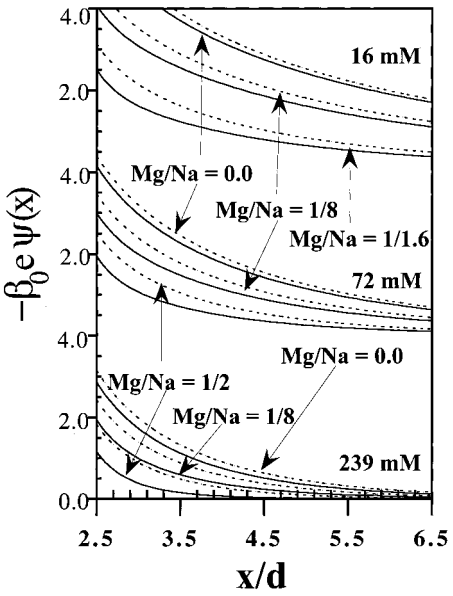

Figure 2. Mean (dimensionless) electrostatic potential around the DNA for 16 mM, 72 mM, and 239 mM NaCl salt with added $MgCl_2$ and various ratios of Mg^{2+} to Na^+. Lines are predictions of the DFT (—) and PB (- - - -) theories. Note that the curves for the two lower concentrations have been shifted in order to fit all three on the same plot.

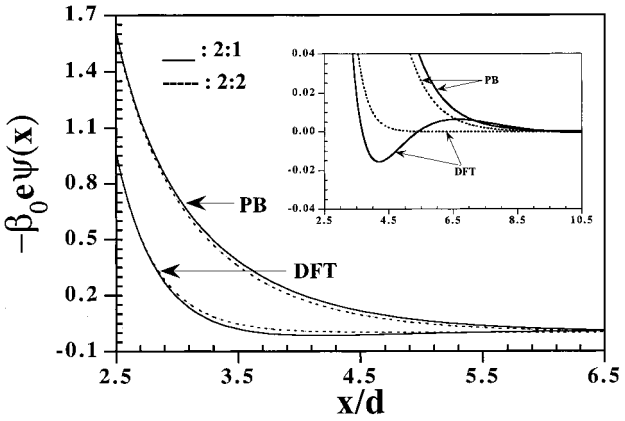

Figure 3. Mean electrostatic potential for pure 2:1 and 2:2 salts around DNA for a bulk concentration of 239 mM from DFT (—) and PB (- - -) theories. The inset shows an expanded view to emphasize the "charge reversal" for the 2:1 salt predicted by the DFT but not by the PB.

An interesting phenomenon in DNA salt systems is the possibility of "charge inversion" where the electrostatic potential becomes positive at some distance even though the polyion is negatively charged. The increased electrostatic attraction between the counterions and the polyion causes a reduction of effective charge of the polyion (DNA), and at high enough concentrations with divalent salts this effective charge sometimes changes sign. This is seen in Figure 3 which depicts DFT and PB predictions for the mean electrostatic potential in 2:1 and 2:2 salts for a concentration of 239 mM. At distances

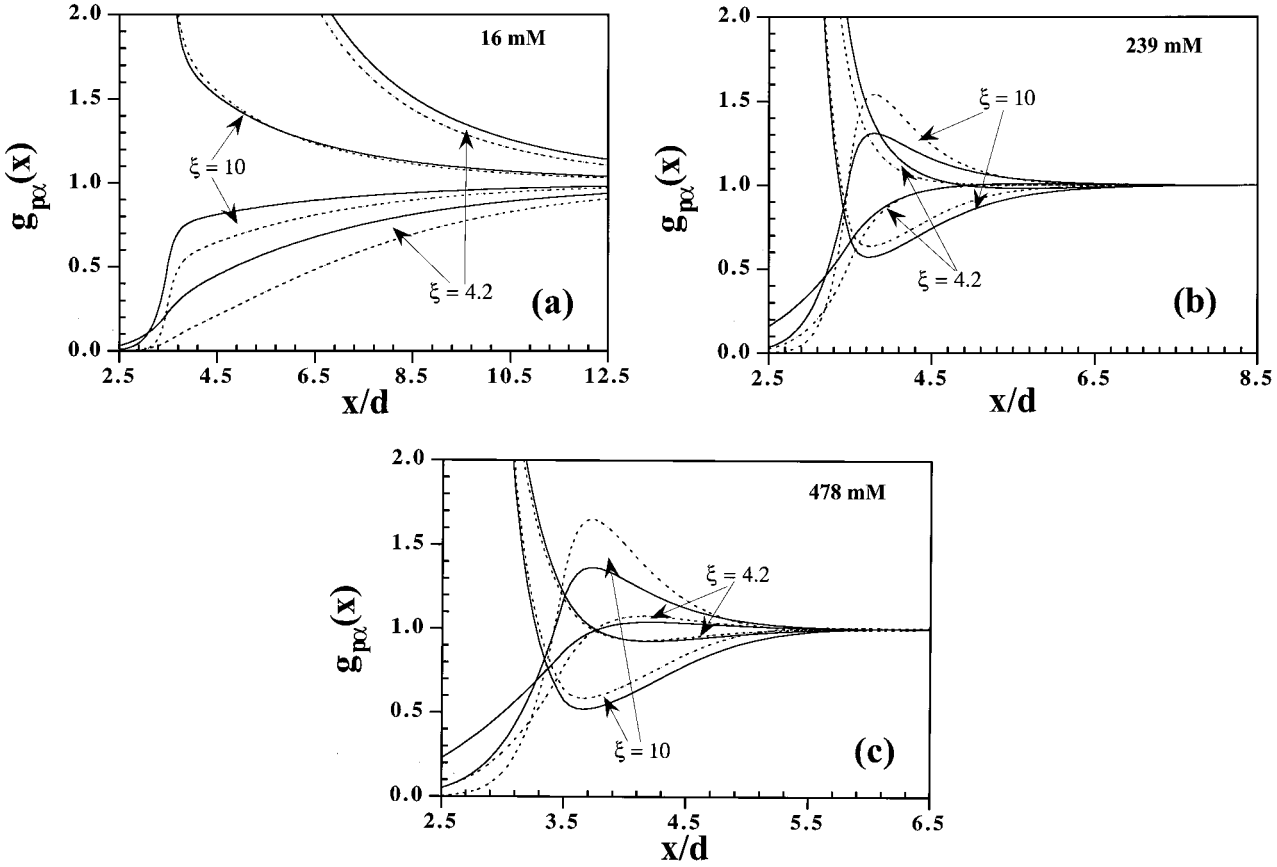

Figure 4. Effect of polyion linear charge density on the polyion small ion pair correlation function. Density functional theory predictions for 2:1 (—) and 2:2 (- - -) salts for concentrations of (a) 16 mM, (b) 239 mM, and (c) 478 mM for two values of the ratio of the Bjerrum length to the average separation between adjacent charges, ξ. Curves with $g_{p\alpha}(x) > 1$ for $x \rightarrow 2.5d$ represent to counterion−polyion pair correlation functions and other curves represent coion−polyion pair correlation functions.

between $3 < x/d < 6.5$ the DFT predicts a positive electrostatic potential, i.e., charge inversion, for the 2:1 but not the 2:2 salt at this concentration. (At higher concentrations the DFT predicts charge inversions for 2:2 salts as well.) The charge inversion is obtained at lower concentrations for the 2:1 salt than in the 2:2 salt because in the former case the counterions have a smaller attraction to the co-ions, resulting in a stronger effective counterion−polyion interaction. The PB theory does not predict any charge inversion at all. Such charge inversion effects are predicted by the modified PB theory[32,33] in some cases.

There is considerably more structure in the pair correlation function between polyion and small ions for high values of the axial charge density, ξ. The results presented so far have been for $\xi = 4.2$ which corresponds roughly to double stranded DNA. There are other systems, such as rodlike tobacco mosaic virus (TMV) colloidal particles, where the axial charge density may be higher. TMV is 300 nm long and is believed to have more than 4000 charged groups on its surface, and for this system $\xi \approx 10$. In Figures 4−6 we compare the DFT and PB approaches for $\xi = 4.2$ and 10.

Figure 4a−c depicts DFT predictions for 2:1 and 2:2 salts, for $\xi = 4.2$ and 10, and for concentrations of 16 mM, 239 mM, and 478 mM, respectively. At the lowest concentration (Figure 4a) the DFT predicts a significant increase in the accumulation of both counterions and co-ions near the charged cylinder. The shape of the pair correlation functions is very different for $\xi = 10$ when compared to $\xi = 4.2$. For higher concentrations (Figures 4b and 4c) the DFT predicts strong inversion effects, i.e., the counterion−polyion $g(x)$ goes through a deep minimum at $x \approx 3.5d$ with a corresponding maximum in the coion−polyion $g(x)$. At larger distances both correlation functions decay monotonically to 1. The strength of the inversion effect is stronger as the concentration is increased. Although the qualitative behavior of the 2:1 and 2:2 salts is similar, in all cases the correlation effects are stronger for the 2:2 salts.

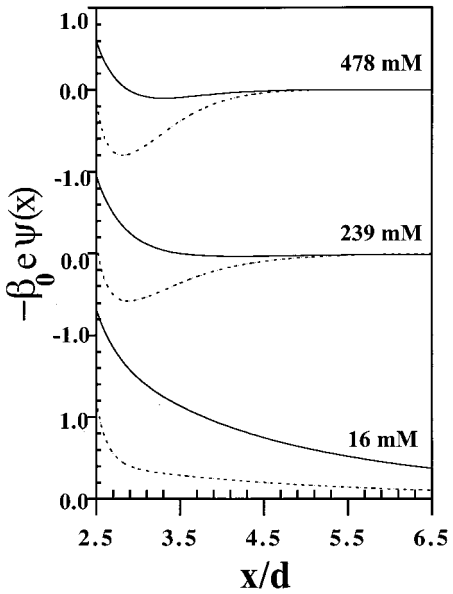

Figure 5. Mean electrostatic potential from the DFT for 2:1 salts for various concentrations (as marked) and for $\xi = 4.2$ (—) and 10 (- - -).

Figure 5 depicts DFT predictions for the mean electrostatic potential for 2:1 salts for the same concentrations as in Figure 4. In all cases, increasing ξ causes the $\psi(x)$ to increase significantly at short distances, as expected. In some cases

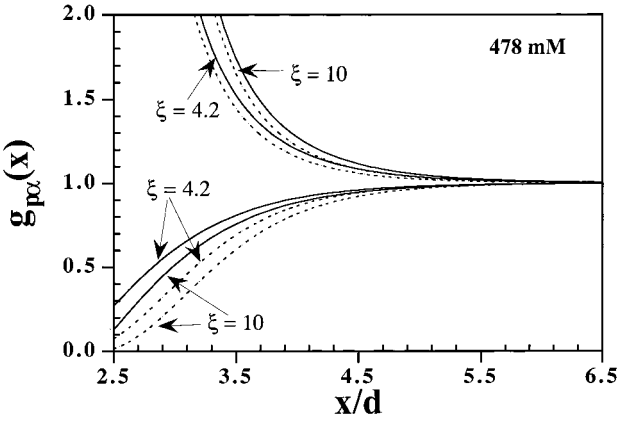

Figure 6. Polyion small ion pair correlation functions from the PB theory for 478 mM. Legend is the same as in Figure 4.

$\psi(x)$ becomes strongly positive, corresponding to significant charge inversion due to correlation effects.

The differences between the DFT and PB theories are significant at high axial charge densities. The PB theory predicts electrostatic potentials and pair correlation functions for $\xi = 10$ that are similar to those for $\xi = 4.2$ and predicts no charge inversion effects at all. Figure 6 depicts the pair correlation functions from the PB theory for 2:1 and 2:2 salts for a concentration of 478 mM to show that the PB predictions are qualitatively different from those of the DFT (see Figure 4c).

IV. Concluding Remarks

We present a density functional approach for the distributions of small ions around a cylindrical polyion. The hard-sphere contribution to the free energy is obtained via a weighted density approximation, and the electrical contribution is calculated through a perturbation with respect to the uniform fluid. The theory is in good agreement with computer simulations for monovalent, divalent, and mixed salts (all with monovalent co-ions). We also compare the theory to predictions of the nonlinear Poisson−Boltzmann approach (PB) and the hypernetted chain (HNC) integral equation theory.

All of the theories are in good agreement with the computer simulation data for axial charge densities corresponding to DNA ($\xi = 4.2$) and pure monovalent salts or high overall salt concentrations. For divalent salts, e.g., $MgCl_2$, the DFT is more quantitatively accurate than the other approaches, especially at low salt concentrations. The qualitative behavior of all theories is similar; however, and all of them provide acceptable predictions of the concentration profiles.

The predictions of the density functional theory are qualitatively different from those of the PB approach for divalent salts (either 2:1 or 2:2) at high concentrations or high polyion charge densities. In this case the DFT predicts charge inversion effects that may be explained in terms of liquid state correlations that are, of course, completely absent from the PB theory. Although these effects are not important in DNA solutions, they could play a significant role in the structure of salt in colloidal systems such as tobacco mosaic virus (TMV) solutions.

The extension of this approach to study the distribution of counterions around realistic double helix DNA is, in principle, straightforward. The basic formulation of the theory will be similar except that one cannot use cylindrical coordinates to simplify the integrals. Similarly, the theory can also be used to investigate two-body and three-body interactions in DNA solutions. Extensions of this nature will be interesting applications and should provide considerable insight into the structure of DNA and TMV solutions.

In summary we have presented a theory that is quantitatively accurate when compared to computer simulations, as easy to implement as the PB approach, and provides a consistent route to the free energy of the system. The theory may be used to calculate, from first principles, the free energy of the ion−polyion system and thus the colligative properties like the activity coefficients and the osmotic coefficients, which are used to characterize the nonideality of polyelectrolyte solutions in presence of salt. This could be important in the study the effect of salt on the nonspecific binding of proteins to DNA.

Acknowledgment. We gratefully acknowledge support from the Alfred P. Sloan Foundation and the National Science Foundation (through Grants CHE 9502320 and CHE 9732604 to A.Y. and CHE 9522057 to the Department of Chemistry). We thank Ms. H. H. Ni, Dr. C. F. Anderson, and Professor M. T. Record, Jr. for providing us with their simulation data prior to publication.

References and Notes

(1) Mandel, M. *Polyelectrolytes*; Reidel: Dordrecht, 1988.
(2) Clementi, E., Sarma, R. H., Eds. *Structure and Dynamics: Nucleic Acids and Proteins*; Adenine: New York, 1983.
(3) Hara, M. *Polyelectrolytes: Science and Technology*; Dekker: New York, 1993.
(4) Beveridge, D. L., Lavery, R., Eds. *Theoretical Biochemistry & Molecular Biophysics*; Adenine: New York, 1991.
(5) Gil Montoro, J. C.; Abascal, J. L. F. *J. Chem. Phys.* **1995**, *103*, 8273; *Mol. Simul.* **1995**, *14*, 313.
(6) Manning, G. S. *Acc. Chem. Res.* **1979**, *12*, 443.
(7) Katchalsky, A. *Pure Appl. Chem.* **1971**, *26*, 327.
(8) Stigter, D. *J. Colloid Interface Sci.* **1975**, *53*, 296.
(9) Manning, G. S. *J. Chem. Phys.* **1969**, *51*, 924; *J. Chem. Phys.* **1969**, *51*, 3249.
(10) Ise, N.; Okubo, T. *Macromolecules* **1978**, *11*, 439.
(11) Manning, G. S. *Biophys. Chem.* **1977**, *7*, 95.
(12) Record, M. T., Jr.; Anderson, C. F.; Lohman, T. M. *Q. Rev. Biophys.* **1978**, *11*, 103.
(13) Brenner, S. L.; McQuarrie, D. A. *J. Theor. Biol.* **1973**, *39*, 343.
(14) Stigter, D. *J. Phys. Chem.* **1978**, *82*, 1603.
(15) Weisbuch, G.; Guéron, M. *J. Phys. Chem.* **1981**, *85*, 517.
(16) Fuoss, R. M.; Katchalsky, A.; Lifson, S. *Proc. Natl. Acad. Sci. U.S.A.* **1951**, *37*, 579.
(17) Katchalsky A.; Alexandrowicz, Z.; Kedem, O. In *Chemical Physics of Ionic Solutions*; Conway, B. E., Barradas, R. G., Eds.; Wiley: New York, 1966.
(18) Marcus, R. A. *J. Chem. Phys.* **1955**, *23*, 1057.
(19) Lifson S.; Katchalsky, A. *J. Polym. Sci.* **1954**, *13*, 43.
(20) Gross, L. M.; Strauss, U. P. In *Chemical Physics of Ionic Solutions*; Conway B. E., Barradas R. G., Eds.; Wiley: New York, 1966.
(21) Sharp, K. A.; Honig, B. *J. Phys. Chem.* **1990**, *94*, 7684.
(22) Anderson, C. F.; Record, M. T., Jr. *Annu. Rev. Phys. Chem.* **1982**, *33*, 191.
(23) Fixman, M. *J. Chem. Phys.* **1979**, *70*, 4995.
(24) Henderson, D., Ed. *Fundamentals of Inhomogeneous Fluids*; Dekker: New York, 1992.
(25) Lozada-Cassou, M. *J. Phys. Chem.* **1983**, *87*, 3279.
(26) Gonzales-Tovar, E.; Lozada-Cassou, M.; Henderson, D. *J. Chem. Phys.* **1985**, *83*, 361.
(27) Yeomans, L.; Feller, S. E.; Sánchez, E.; Lozada-Cassou, M. *J. Chem. Phys.* **1993**, *98*, 1436.
(28) Bacquet, R.; Rossky, P. J. *J. Phys. Chem.* **1984**, *88*, 2660; *J. Phys. Chem.* **1988**, *92*, 3604.
(29) Bailey, J. M. *Biopolymers* **1973**, *12*, 1705.
(30) Iwasa, K.; McQuarrie, D. A.; Kwak, J. C. T. *J. Phys. Chem.* **1978**, *82*, 1979.
(31) Skolnick, J. *Macromolecules* **1979**, *12*, 515.
(32) Das, T.; Bratko, D.; Bhuiyan, L. B.; Outhwaite, C. W. *J. Phys. Chem.* **1995**, *99*, 410.
(33) Das, T.; Bratko, D.; Bhuiyan, L. B.; Outhwaite, C. W. *J. Chem. Phys.* **1997**, *107*, 9197.
(34) Bratko, D.; Vlachy, V. *Chem. Phys. Lett.* **1982**, *90*, 434.
(35) LeBret, M.; Zimm, B. H. *Biopolymers* **1984**, *23*, 271.

(36) Murthy, C. S.; Bacquet, R. J.; Rossky, P. J. *J. Phys. Chem.* **1985**, *89*, 701.
(37) Mills, P.; Anderson, C. F.; Record, M. T., Jr. *J. Phys. Chem.* **1985**, *89*, 3984.
(38) Vlachy, V.; Haymet, A. D. J. *J. Chem. Phys.* **1986**, *84*, 5874.
(39) Mills, P.; Anderson, C. F.; Record, M. T., Jr. *J. Phys. Chem.* **1986**, *90*, 6541.
(40) Hohenberg, P.; Kohn, W. *Phys. Rev. B* **1964**, *136*, 864.
(41) Percus, J. K. In *The Equilibrium Theory of Classical Fluids; A Lecture Note and Reprint Volume*; Frisch, H. L., Lebowitz, J. L., Eds.; Benjamin: New York, 1984.
(42) Hansen, J. P.; McDonald, I. R. *Theory of Simple Liquids*; Academic: London, 1986.
(43) Ramakrishnan, T. V.; Youssouff, M. *Phys. Rev. B* **1979**, *19*, 2775.
(44) Evans, R. In *Fundamentals of Inhomogeneous Fluids*; Henderson, D., Ed.; Dekker: New York, 1992.
(45) Mier-y-Teran, L.; Suh, S. H.; White, H. S.; Davis, H. T. *J. Chem. Phys.* **1990**, *92*, 5087.
(46) Patra, C. N.; Ghosh, S. K. *Phys. Rev. E* **1993**, *47*, 4088.
(47) Tang, Z.; Scriven, L. E.; Davis, H. T. *J. Chem. Phys.* **1992**, *96*, 4639.
(48) Patra, C. N.; Ghosh, S. K. *J. Chem. Phys.* **1997**, *106*, 2752.
(49) Tarazona, P. *Phys. Rev. A* **1985**, *31*, 2672.
(50) Denton, A. R.; Ashcroft, N. W. *Phys. Rev. A* **1989**, *39*, 426.
(51) Tang, Z.; Mier-y-Teran, L.; Davis, H. T.; Scriven, L. E.; White, H. S. *Mol. Phys.* **1990**, *71*, 369.
(52) Patra, C. N.; Ghosh, S. K. *J. Chem. Phys.* **1994**, *100*, 5219.
(53) Yethiraj, A.; Woodward, C. E. *J. Chem. Phys.* **1995**, *102*, 5449.
(54) Denton, A. R.; Ashcroft, N. W. *Phys. Rev. A* **1991**, *44*, 8242.
(55) Waisman, E.; Lebowitz, J. L. *J. Chem. Phys.* **1972**, *56*, 3086, 3093.
(56) Ornstein, L. S.; Zernike, F. *Proc. Acad. Sci. Amsterdam* **1914**, *17*, 793.
(57) Attard, P. *Adv. Chem. Phys.* **1996**, *92*, 1.
(58) Ichiye, T.; Haymet, A. D. J. *J. Chem. Phys.* **1988**, *89*, 4315.
(59) Ni, H. H.; Anderson, C. F.; Record, M. T., Jr. *J. Phys. Chem. B* **1999**, *103*, 3489.